Chapter 6

Ratio of the diffractive to the non-diffractive $b\bar{b}$ production

The number of $b\bar{b}$ events in both the whole electron sample and the diffractive candidates are estimated in the previous chapter. In this chapter, we calculate the ratio of the diffractive to the non-diffractive $b\bar{b}$ production $R_{b\bar{b}}$ using these results. At first we describe the correction factors due to the limited acceptance of the rapidity gap method which is used to select the diffractive candidates from the whole electron sample. The ratio $R_{b\bar{b}}$ is then calculated. The systematic uncertainties on $R_{b\bar{b}}$ are estimated in the final section.

6.1 Acceptance for the rapidity gap tagging

6.1.1 Acceptance for single interaction events

The efficiency of the rapidity gap tagging is limited to the events with only one $p\bar{p}$ interaction in a single bunch crossing although we allow the events to have multiple reconstructed vertex in the VTX. The reason for this inefficiency is the following: when the extra $p\bar{p}$ interactions occur in a single bunch crossing, generated particles from these interactions always kill the rapidity gap signal. The acceptance for the single interaction is evaluated as a function of the luminosity.

The mean luminosity for a single bunch crossing $\langle L_{bunch} \rangle$ is calculated with an instantaneous luminosity L_{inst} measured by the BBC hit rate,

$$\begin{aligned}\langle L_{bunch} \rangle =& \frac{C_{acc} \times \langle L_{inst} \rangle}{f} \\ =& \frac{0.9772 \times 8.415}{286.278} \\ =& 0.02872(mb^{-1}) \\ \left(C_{acc} =& 1 - 0.002704 \times \langle L_{inst} \rangle \right)\end{aligned}$$

where C_{acc} is the accidental correction factor [35] for L_{inst} and f is the frequency of a bunch crossing in the Tevatron.

Using the above $\langle L_{bunch} \rangle$, the average number of inelastic $p\bar{p}$ interactions in a single bunch crossing is given by,

$$\begin{aligned}\langle n \rangle =& \sigma_{BBC} \times \langle L_{bunch} \rangle \\ =& 51.15 \times 0.02872 \\ =& 1.469\end{aligned}$$

where σ_{BBC} is the cross section of an inelastic $p\bar{p}$ interaction which hits the BBC [35, 40]. Finally, the acceptance for events without extra visible interactions is given by the Poisson statistics,

$$\begin{aligned}A_{1vx} =& e^{-\langle n \rangle} \\ =& 0.230.\end{aligned}$$

6.1.2 Livetime efficiency of the BBC and the forward calorimeter

Any noises in the BBC or the forward calorimeters kill the rapidity gap signal. The no-noise probability of the BBC and the forward calorimeters is estimated by studying a rate of noise hits in those detectors for events with no reconstructed vertex in the VTX. Although our analysis is done for RUN1B data, we use RUN1A clock trigger data to study this efficiency

because there are no such unbiased triggers in RUN1B. Figure 6.1 shows a probability of no-noise in the forward detectors plotted as a function of an instantaneous luminosity. The noise associated with the luminosity is observed in the plot. We parameterize the luminosity dependence of the noise using a linear function and then estimate the probability of no-noise in our RUN1B electron sample. The probability of no-noise is 0.805 and 0.739 for $-\eta$ side and $+\eta$ side, respectively. Since the number of observed rapidity gap signals are the same in each sides (see Sec. 3.2), we take the mean of two numbers for the probability of no-noise in our sample,

$$A_{live} = 0.772.$$

6.1.3 Gap acceptance for diffractive events

The acceptance for the rapidity gap tagging for the diffractive $b\bar{b}$ event is evaluated using `POMPYT 2.6` Monte Carlo simulator [36]. `POMPYT 2.6` is an add-on program of the `PYTHIA 5.7`. The simulation is based on the Ingelman-Shelin model as described in Chapter 1. The `POMPYT 2.6` employs the following steps for the event generation. At first, "pomeron" having the momentum of 900ξ GeV/c is emitted from the beam particle. The kinematical parameters of the pomeron (t, ξ) are randomly determined according to the Donnachie-Landshoff flux, where ξ is the fractional momentum of the pomeron carrying to the proton and t is a momentum transfer squared. We use the following parameters in the DL flux model,

$\beta^0 = 3.202\ \mathrm{GeV}^{-1}$	effective quark – pomeron coupling
$\epsilon' = 0.115$	intercept of the pomeron trajectory
$\alpha' = 0.26\ \mathrm{GeV}^{-2}$	slope of the pomeron trajectory
$\sigma_T^{p\mathbb{P}} = 2.3$ mb	pomeron – proton total cross section

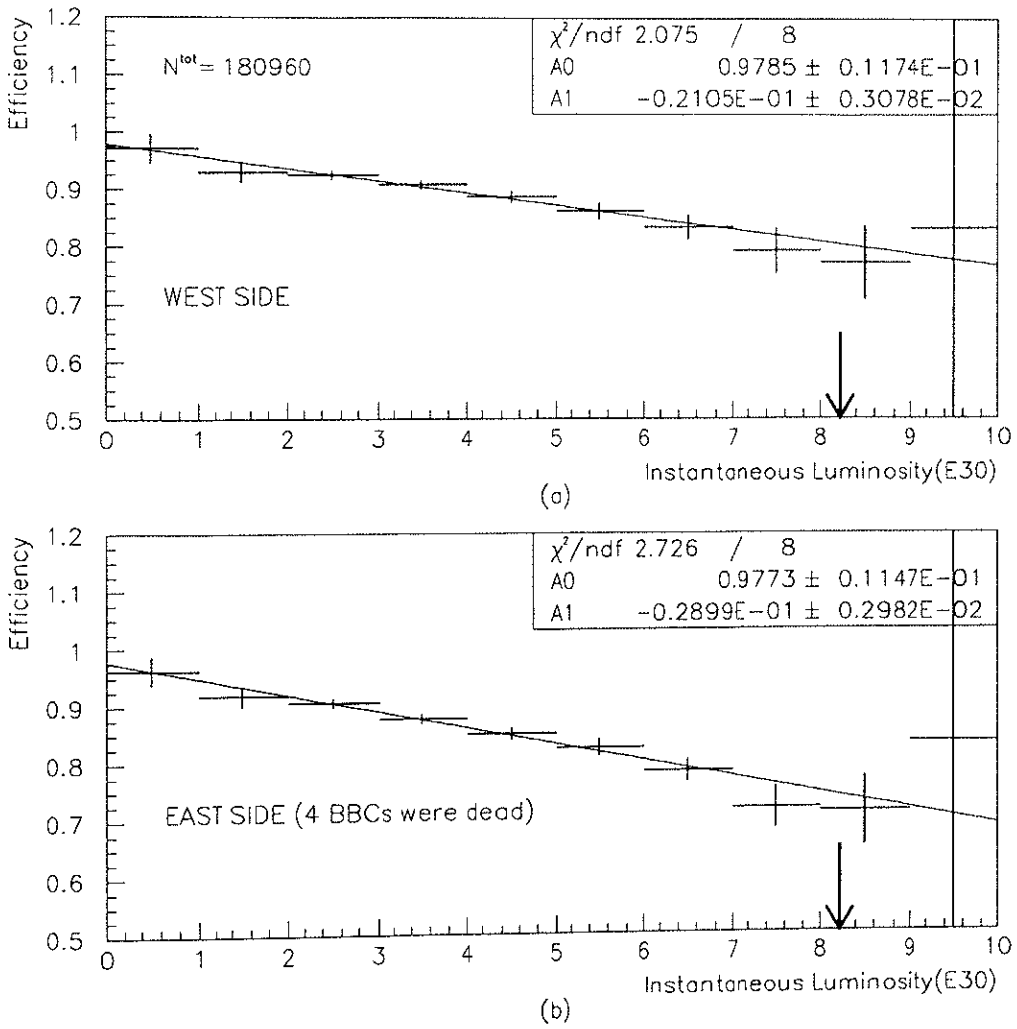

Figure 6.1: The probability of no-noise in both BBC and forward calorimeters as a function of instantaneous luminosity($\times 10^{30}$). The arrow points to the mean instantaneous luminosity of the whole electron sample (RUN1B). (a) The probability of no-noise in west side ($\eta < 0$) detectors. (b) The probability of no-noise in east side ($\eta > 0$) detectors.

Next the hard collision between the partons in the pomeron and the target particle is simulated using the leading order perturbative QCD calculation with the PYTHIA 5.7. We use the EHLQ set-1 structure function to simulate the parton density in the proton as used in the previous CDF studies for the diffractive W [11] and the diffractive dijet production [10]. The fragmentation process of the outgoing partons are simulated with the JETSET 7.4.

We use the two kinds of the structure function, "flat" distribution ($zf_{g,q/I\!P}(z) \sim 1$) and "hard" distribution ($zf_{g,q/I\!P}(z) \sim z(1-z)$) for the pomeron. The kinematical ranges of the event generation is limited for ξ below 0.1 and $|t|$ below 5.0 GeV$^2/c^2$. The b-quarks are generated with p_T above 12 GeV/c. The restriction to the semi-leptonic decay and the simulation of the CDF detector including the Level-2 trigger are made as described in Sec. 5.1. The simulated events are filtered using the same selection cuts as described in Chapter 3 except for the CPR charge requirement.

Using the filtered sample, the particle multiplicity at the location of the forward detectors is further simulated using the full detector simulation program CDFSIM which simulates the interactions in the detector material. The output signal from the detector for the low energy particles is not correctly modeled in the CDFSIM and QFL. Instead of these simulators, we simply model the response of the forward calorimeter by the following equation,

$$E_i^{obs} = S_i \times p^{gen} + C_i$$

where p^{gen} is a momentum of the particle, S_i and C_i are energy correction factors determined as a function of each η of the tower. The detail of this model is described in Appendix C.

The final results of the multiplicity simulations are shown in Figs. 6.2(a)-(d) for the four kinds of pomeron model, flat-gluon, flat-quark, hard-gluon, and hard-quark, respectively. The acceptance for the rapidity gap tagging,

N_{BBC}=0 and N_{clust}=0, is found to be,

$$A_{gap}^{FG} = 0.412, \quad \text{(Flat Gluon pomeron)}$$
$$A_{gap}^{FQ} = 0.273, \quad \text{(Flat Quark pomeron)}$$
$$A_{gap}^{HG} = 0.359, \quad \text{(Hard Gluon pomeron)}$$
$$A_{gap}^{HQ} = 0.217. \quad \text{(Hard Quark pomeron)}$$

The kinematic variable $\xi(< 1)$ is related to the size of rapidity gap $\Delta\eta$ by the following equation,

$$\Delta\eta \sim -\ln\xi.$$

The size of the rapidity gap increases as the pomeron ξ decrease. Figures 6.3(a)-(d) show the ξ distributions of the simulated events. The events tagged by a rapidity gap is populated in the ξ range below 0.1.

6.2 Ratio of the diffractive to the non-diffractive $b\bar{b}$ production

The number of $b\bar{b}$ events found in the diffractive signal region is $N_{b\bar{b}}(0,0) = 44.4 \pm 10.2$ events as described in Sec. 3.2.

Since this number contains the contribution of the non-diffractive $b\bar{b}$ events, we have to remove this contribution at first. The non-diffractive events in the diffractive signal region is $N^{ND}(0,0) = 24.4$ events as described in Sec. 3.2. Assuming that the fraction of $b\bar{b}$ events in the non-diffractive sample does not depend on the forward multiplicity, we obtain the number of the $b\bar{b}$ events in the above backgrounds,

$$\begin{aligned} N_{b\bar{b}}^{ND}(0,0) &= N^{ND}(0,0) \times f_{b\bar{b}}^{ND} \\ &= 24.4 \times (0.454 \pm 0.003) \\ &= 11.1 \pm 0.08(stat) \text{ events.} \end{aligned}$$

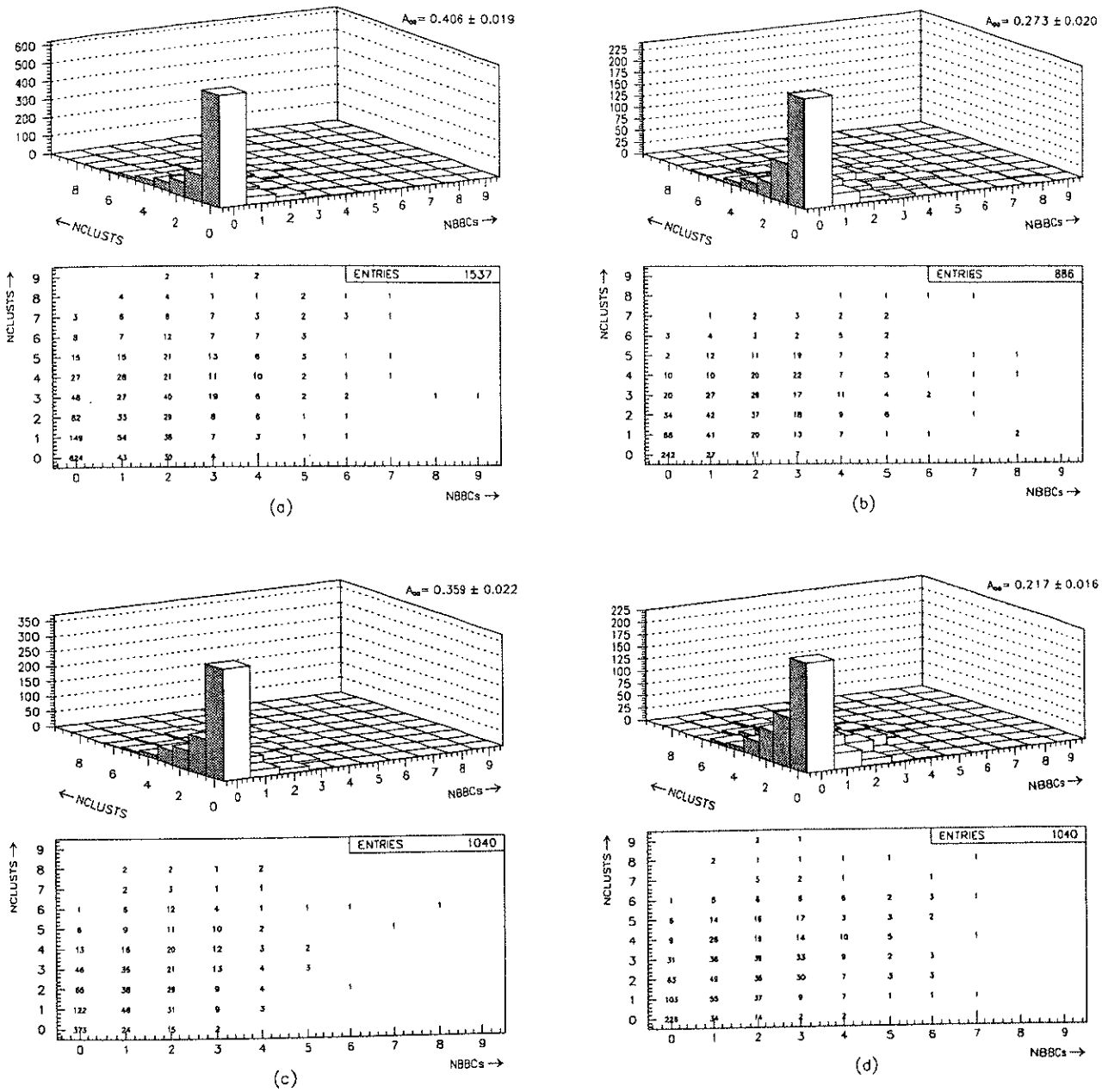

Figure 6.2: Simulated multiplicity distribution for the diffractive $b\bar{b}$ events with (a) flat-gluon pomeron, (b) flat-quark pomeron, (c) hard-gluon pomeron, and (d) hard-quark pomeron.

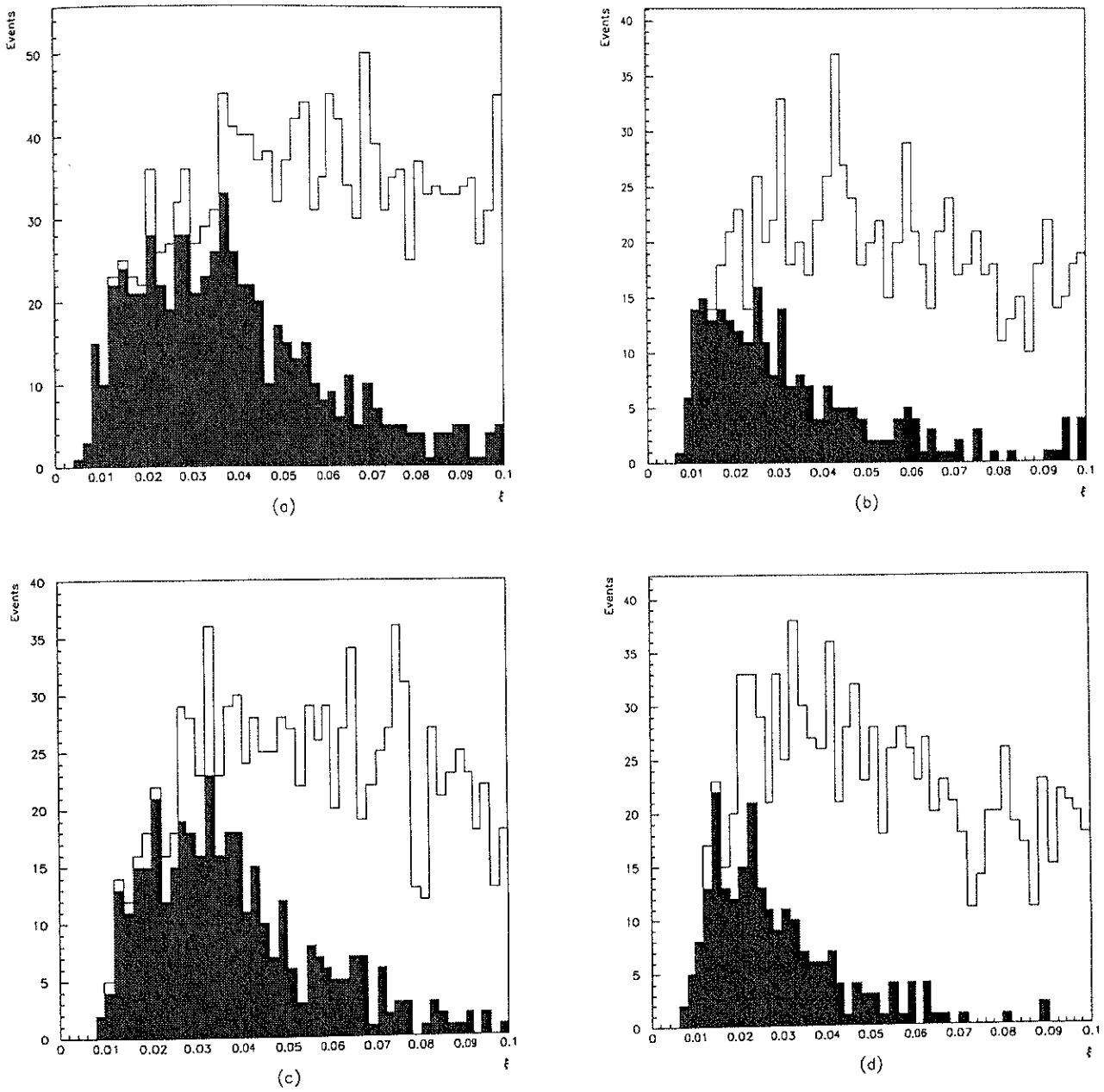

Figure 6.3: Simulated ξ distribution for the diffractive $b\bar{b}$ events. Shaded area shows the events tagged by a rapidity gap in the forward detectors with (a) flat-gluon pomeron, (b) flat-quark pomeron, (c) hard-gluon pomeron, and (d) hard-quark pomeron.

The number of diffractive $b\bar{b}$ events in the signal region is found to be 33.3±10.2(stat).

The total number of diffractive $b\bar{b}$ events in the whole electron sample is calculated by correcting the acceptances,

$$\begin{aligned} N_{b\bar{b}}^{DIF}(\xi < 0.1; \mathrm{FG}) &= \left\{ N_{b\bar{b}}(0,0) - N_{b\bar{b}}^{ND}(0,0) \right\} \times \frac{1}{A_{1vx}} \times \frac{1}{A_{live}} \times \frac{1}{A_{gap}^{FG}} \\ &= (33.3 \pm 10.2) \times \frac{1}{0.230} \times \frac{1}{0.772} \times \frac{1}{0.406} \\ &= 461 \pm 142(stat) \text{ events.} \end{aligned}$$

The total number of $b\bar{b}$ events in the whole electron sample is 73371±485(stat) events. The ratio of the diffractive to the non-diffractive $b\bar{b}$ production is obtained,

$$\begin{aligned} R_{b\bar{b}}(\xi < 0.1; \mathrm{FG}) &= \frac{N_{b\bar{b}}^{DIF}(\xi < 0.1; \mathrm{FG})}{N_{b\bar{b}}^{ND}} = \frac{461 \pm 142}{73371 \pm 485} \\ &= 0.63 \pm 0.19(stat)\% \end{aligned}$$

Since the gap acceptance is a model dependent quantity, we show here the result without correcting the gap acceptance,

$$R_{b\bar{b}}(\mathrm{GAP}) = 0.255 \pm 0.078(stat)\%$$

where "GAP" means no energy deposition above 1.5 GeV in the forward calorimeter ($2.4 < |\eta| < 4.2$) and no charged particle hit in the BBC ($3.2 < |\eta| < 5.9$).

The ratio of the diffractive to the non-diffractive $b\bar{b}$ events after the gap acceptance correction is listed for each pomeron models below,

$$\begin{aligned} \mathrm{Flat-Gluon}: &\ R_{b\bar{b}}(\xi < 0.1; \mathrm{FG}) = 0.63 \pm 0.19(stat)\% \\ \mathrm{Flat-Quark}: &\ R_{b\bar{b}}(\xi < 0.1; \mathrm{FQ}) = 0.93 \pm 0.29(stat)\% \\ \mathrm{Hard-Gluon}: &\ R_{b\bar{b}}(\xi < 0.1; \mathrm{HG}) = 0.71 \pm 0.22(stat)\% \\ \mathrm{Hard-Quark}: &\ R_{b\bar{b}}(\xi < 0.1; \mathrm{HQ}) = 1.18 \pm 0.36(stat)\%. \end{aligned}$$

6.3 Systematic uncertainties

We have measured the $b\bar{b}$ fraction in the whole electron sample using two independent methods, the ${p_T}^{rel}$ fit and the impact parameter fit. The difference in the $b\bar{b}$ fractions between the two methods is 10.6% relative to the combined result of the measurements. We assign this difference as a systematic uncertainty on the $b\bar{b}$ fraction for the whole electron sample.

$$\left.\frac{\delta R_{b\bar{b}}}{R_{b\bar{b}}}\right|_{b\bar{b}(ND)} = \frac{\delta N_{b\bar{b}}^{ND}}{N_{b\bar{b}}^{ND}} = 0.106$$

We also assign this relative uncertainty of 10.6% as the systematic uncertainty on the $b\bar{b}$ fraction in the diffractive candidates.

$$\begin{aligned}\left.\frac{\delta R_{b\bar{b}}}{R_{b\bar{b}}}\right|_{b\bar{b}(0,0)} &= \frac{\delta N_{b\bar{b}}(0,0)}{N_{b\bar{b}}^{DIF}(0,0)} = \frac{0.106 \times 44.4}{33.3} \\ &= 0.141\end{aligned}$$

The method to estimate the non-diffractive background in the diffractive candidates was described in Sec. 3.2. We use the uncertainty in the background fitting as a systematic uncertainty.

$$\begin{aligned}\left.\frac{\delta R_{b\bar{b}}}{R_{b\bar{b}}}\right|_{BG} &= \frac{\delta N_{b\bar{b}}^{ND}(0,0)}{N_{b\bar{b}}^{DIF}(0,0)} = \frac{24.40 \times 0.454}{33.3} \\ &= 0.076\end{aligned}$$

The systematic uncertainty due to the single interaction acceptance is calculated using the σ_{BBC} uncertainty of 1.7mb [40].

$$\begin{aligned}\left.\frac{\delta R_{b\bar{b}}}{R_{b\bar{b}}}\right|_{1vx} &= \frac{\delta A_{1vx}}{A_{1vx}} = \langle L_{bunch} \rangle \times \delta(\sigma_{BBC}) \\ &= 0.049\end{aligned}$$

We measure the livetime efficiency of the BBC and the forward calorimeter using RUN1A "empty" events, but the BBC condition in RUN1A is not identical to that in RUN1B since four BBC modules are dead in RUN1A while they are alive in RUN1B. On the other hand, the BBC in the west side

is kept in the same condition through RUN1A and RUN1B. The difference in measured efficiencies between the east side and the west side is 0.066. We assign this difference as a systematic uncertainty on the live time efficiency of the BBC and the forward calorimeter.

$$\left.\frac{\delta R_{b\bar{b}}}{R_{b\bar{b}}}\right|_{live} = \frac{\delta A_{live}}{A_{live}} = \frac{0.066}{0.772} = 0.086$$

The systematic uncertainty due to the gap acceptance for the diffractive events depends on the model of the Monte Carlo program and the forward detector simulation. We restrict our study in the models where the pomeron has a flat structure function, $zf_{g,q/I\!P}(z) \sim 1$ or a hard structure function, $zf_{g,q/I\!P}(z) \sim z(1-z)$. We estimate the uncertainty due to the detector simulation by changing the energy correction factors and offsets according to the fitting errors. We found this uncertainty to be $\pm 1.5\%$. Taking a quadratic sum of the statistical uncertainty for the Monte Carlo events and this uncertainty, we obtain the systematic uncertainty on the Monte Carlo gap acceptance as:

$$\left.\frac{\delta R_{b\bar{b}}}{R_{b\bar{b}}}\right|_{gap(FG)} = \frac{\delta A_{gap(FG)}}{A_{gap(FG)}} = \frac{\sqrt{0.015^2 + 0.019^2}}{0.406} = 0.059$$

$$\left.\frac{\delta R_{b\bar{b}}}{R_{b\bar{b}}}\right|_{gap(FQ)} = 0.082$$

$$\left.\frac{\delta R_{b\bar{b}}}{R_{b\bar{b}}}\right|_{gap(HG)} = 0.078$$

$$\left.\frac{\delta R_{b\bar{b}}}{R_{b\bar{b}}}\right|_{gap(HQ)} = 0.090$$

Including all systematic uncertainties, the ratio of the diffractive to the

non-diffractive $b\bar{b}$ production is measured as:

$$R_{b\bar{b}}(\xi < 0.1; \mathrm{FG}) = 0.63 \pm 0.19(stat) \pm 0.14(syst)\%$$

$$R_{b\bar{b}}(\xi < 0.1; \mathrm{FQ}) = 0.93 \pm 0.29(stat) \pm 0.22(syst)\%$$

$$R_{b\bar{b}}(\xi < 0.1; \mathrm{HG}) = 0.71 \pm 0.22(stat) \pm 0.16(syst)\%$$

$$R_{b\bar{b}}(\xi < 0.1; \mathrm{HQ}) = 1.18 \pm 0.36(stat) \pm 0.27(syst)\%$$

All systematic uncertainties discussed in this section are listed in Table 6.1.

The number of $b\bar{b}$ events in the whole electron sample	10.6%
The number of $b\bar{b}$ events in (0,0)	14.1%
The number of non-diffractive $b\bar{b}$ events in (0,0)	7.6%
Acceptance for single interaction	4.9%
Live time efficiency for the forward detectors	8.6%
Monte Carlo gap acceptance	5.9%
Total systematic uncertainty	22.3%

Table 6.1: Systematic uncertainties relative to the $R_{b\bar{b}}$ for the flat-gluon pomeron model.